

Production of Slow π^+ Mesons in Photographic Emulsion Nuclei by 660 mev Protons*

V. V. ALPERS,** L. M. BARKOV, R. I. GERASIMOVA,
I. I. GUREVICH, A. P. MISHAKOVA, K. N. MUKHIN
AND B. A. NIKOL'SKII

(Submitted to JETP editor Feb. 11, 1956)

J. Exptl. Theoret. Phys. (U.S.S.R.) 30, 1034-1039 (June, 1956)

Production of slow mesons by 660 mev protons was studied with the aid of the emulsion camera. The method employed permitted us to study effectively the stars formed by π^- mesons as well as the energy and angular spectra of the slow π^+ mesons formed in nuclei.

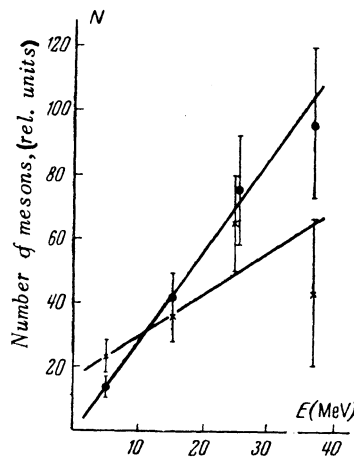
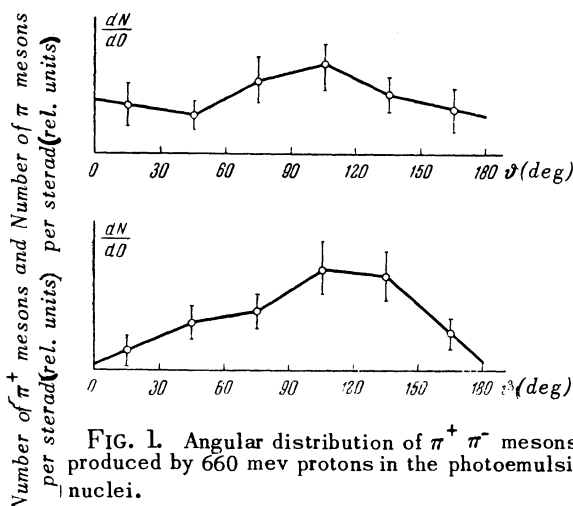
The present work is a continuation of the study of formation of π^+ and π^- mesons in the nuclei of photoemulsions by fast nucleons and contains results obtained with 660 mev protons. The camera used in this work was prepared with the photoemulsion NIKFI, type R (85% Ag Br), containing 45 layers each 300 μ thick and 42 mm in diameter and was irradiated with 600 ± 10 mev protons obtained from the synchrocyclotron of the Institute for Nuclear Problems, Academy of Sciences, USSR.

The greater thickness of the emulsion camera (15 mm) and the higher sensitivity of the emulsion used in this work permitted a more detailed analysis of the process of formation of slow π^- mesons in the photoemulsion nuclei.

I. ENERGY AND ANGULAR DISTRIBUTIONS OF THE FORMED π MESONS

To obtain a correct picture of the different characteristics of the π^+ and π^- mesons in the photoemulsion we used the method of following each meson track from its end to the point of π meson production or its entrance to the camera. There were found by this method 95 cases of π^+ meson and 80 cases of π^- meson production. After making corrections for the end effect (as discussed in Ref. 1) there were obtained the angular distribution and energy spectrum of the produced π^+ and π^- mesons.

In Fig. 1 are shown the angular distributions of π^+ and π^- mesons produced by 600 mev protons in the photoemulsion nuclei. It is seen from Fig. 1 that the π meson production cross section depends slightly on the flight angle relative to the direction of the beam of the incident particles. The energy distribution of the π^+ and π^- mesons is shown in Fig. 2. It is seen from Fig. 2 that the difference between the spectra of π^+ and π^- mesons produced by protons is preserved at 660 mev although it is less pronounced than at 460 mev (Ref. 1) which is possibly connected with the increasing effect of the charge redistribution between the captured nucleon and the nucleus prior to the formation of the meson.



*This communication is based on results obtained during 1954-55.

**Deceased

There was also computed the ratio of π^+ to π^- meson production which for mesons of $E_\pi > 40$ mev, after corrections for the end effect, turned out to be $\pi^+/\pi^- = 1.6 \pm 0.4$. Allowance for the Coulomb displacement of 15 mev (Ref. 1) in the π^+ and π^- mesons energy spectra yields for the value of this ratio the quantity $\pi^+/\pi^- = 2.3 \pm 0.5$ which coincides, within the limits of error, with the results obtained by irradiation of emulsions with 460 mev protons:

$$\pi^+/\pi^- = 2.5 \pm 0.6.$$

The production cross sections of π^+ and π^- mesons of energy $E_\pi < 40$ mev by 660 mev protons in photoemulsion nuclei was obtained from the number of produced π mesons in a definite volume of the emulsion and the density of the proton beam (Ref. 1). The cross sections were found to be: $\sigma_{\pi^-} = (2.8 \pm 1.0) \cdot 10^{-27} \text{ cm}^2$; $\sigma_{\pi^+} = (4.4 \pm 1.5) \cdot 10^{-27} \text{ cm}^2$; $\sigma_{(\pi^+\pi^-)} = (7.2 \pm 1.8) \cdot 10^{-27} \text{ cm}^2$. These cross sections refer to mesons of the energy interval $0 < E_\pi < 40$ mev.

2. ANALYSIS OF STARS ACCOMPANYING PRODUCTION OF π MESONS

In the analysis of the stars accompanying production of π mesons, traces of the particles leaving the star were examined up to the point where they were stopped in the emulsion camera, or up to their emergence from it. In the first case the energy was

determined from the curves $E = f(R)$ where R denotes the ionization path of the particle; in the second case, the energy was determined from the curves of energy dependence on the grain density $E = f(dN/dR)$. The curve $E = f(dN/dR)$ was obtained experimentally for π mesons and recomputed for protons according to the formula

$$\frac{dN}{dR}(E_p) = \frac{dN}{dR} \left(\frac{E_\pi M_p}{M_\pi} \right).$$

The application of this method permitted more reliable measurements of the energies of particles emitted from the stars compared with other investigations in which photographic plates were used for this purpose.

A total of 95 stars accompanied by production of π^+ mesons and 80 stars by production of π^- mesons were analyzed, and not a single case of formation of pairs of mesons was registered in all the 175 cases. In addition, we investigated 74 stars found in following tracks of protons not containing π mesons (see Sec. 3).

The distribution according to energy of the particles leaving the stars is shown in Fig. 3. The photographic emulsion used in the work did not permit effective identification of protons and α -particles of low energy ($E_p < 40$ mev); the particle energy in all cases was therefore determined from the curves $E = f(R)$ for protons. Numerical values for the energy distributions of the particles are shown in Table 1.

TABLE I

Average star energy \bar{E} (combined kinetic energy of charged particles) and average number of charged particles \bar{N} in stars with and without production of mesons

Particle energy (in mev)		0-30	30-100	>100	All energies
E	π^+	18±2	23±4	143±19	184±13
	π^-	28±2	54±7	163±22	246±17
	without π	28±2	36±5	296±34	360±20
N	π^+	1.85±0.14	0.4 ±0.07	0.63±0.08	2.9 ±0.17
	π^-	3.2 ±0.2	0.9 ±0.1	0.71±0.09	4.85±0.25
	without π	2.5 ±0.2	0.62±0.09	1.0 ±0.1	4.2 ±0.2

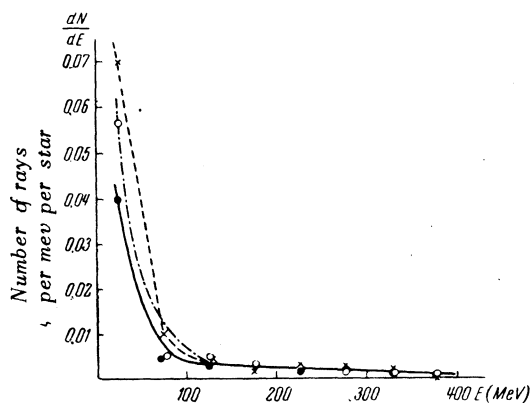


FIG. 3. Energy distribution of particles leaving the stars under the action of 660 mev protons. ●—denotes stars with production of π^+ mesons; ×—stars with production of π^- mesons; O—stars without any mesons.

As shown in Table 1, the number of fast protons leaving the stars ($E > 100$ mev) is substantially the same for all cases of π^+ and π^- meson production, but there is a difference in the number of charged particles of low and medium energy. The independence of the number of fast protons of the sign of the produced meson is maintained also for the case when the meson is emitted forward. The latter characteristic, pointed out in the analysis of stars produced by 400-460 mev nucleons, indicates that the nuclei are transparent to slow mesons ($E_\pi < 40$ mev) and that there exists a high probability of the nucleons recharging in the nucleus.

Stars which are not accompanied by π meson production are characterized by a relatively high number of charged particles and by high average value of star energy E . The difference in the number of charged particles of small and medium energies ($E < 100$ mev) corresponds to the change in the nuclear charge with the production of mesons of different signs.

In Figs. 4 and 5 are shown angular distributions of slow ($E < 30$ mev) and fast ($E > 100$ mev) particles leaving the stars. The corresponding numerical characteristics are shown in Table 2 where the anisotropy is determined as

$$\frac{[N(0 \div 90^\circ) - N(90 \div 180^\circ)]}{[N(0 \div 90^\circ) + N(90 \div 180^\circ)]}$$

It should be noted that the anisotropy of the angular distribution of particles leaving the stars

is maintained down to particles of lowest energies. The corresponding results are shown in Fig. 6. It can be readily shown that the observed anisotropy cannot be explained by the motion of the nucleus as a whole.

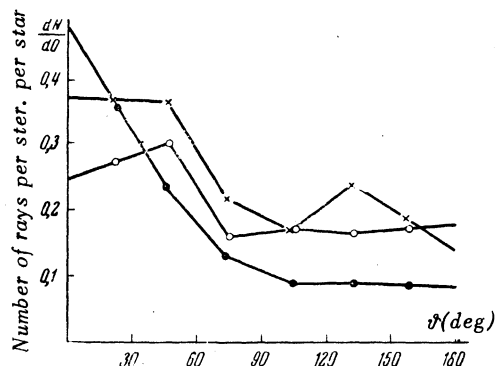


FIG. 4. Angular distribution of slow ($E < 30$ mev) particles leaving the stars under the action of 660 mev protons. ●—denotes stars with the production of π^+ mesons; ×—stars with production of π^- mesons; O—stars without mesons.

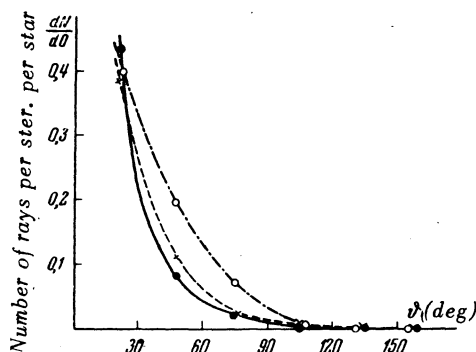


FIG. 5. Angular distribution of fast ($E > 100$ mev) particles leaving the stars under the action of 660 mev protons. ●—denotes stars with production of π^+ mesons; ×—stars with production of π^- mesons; O—stars without mesons.

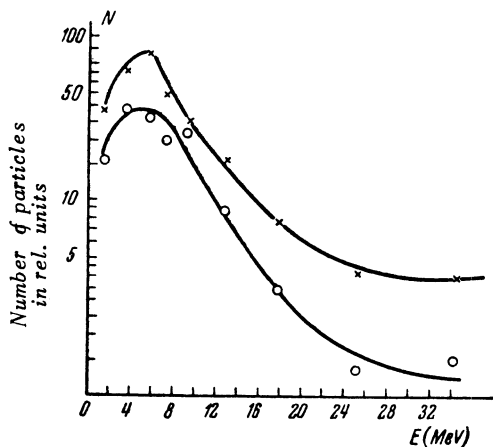


FIG. 6. Distribution by energy of slow particles ($E < 20$ mev) emitted forward ($\vartheta < 90^\circ$) and backward ($\vartheta > 90^\circ$) relative to the beam of the incident 660 mev protons. \times - denotes particles emitted forward ($0^\circ < \vartheta < 90^\circ$) from stars with the production of π^+ and π^- mesons; o - particles emitted backward ($90^\circ < \vartheta < 180^\circ$) from stars with the production of π^+ and π^- mesons.

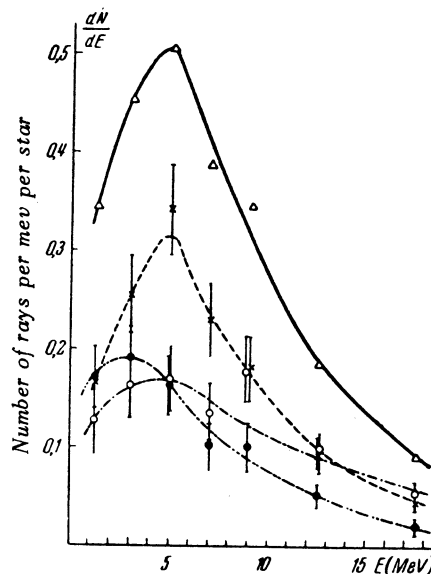


FIG. 7. Distribution by energy of slow particles ($E < 20$ mev) leaving the stars under the action of 660 mev protons. \times - denotes stars with the production of π^+ mesons; o - stars without mesons; Δ - all the stars (in relative units); \bullet - stars with the production of π^+ mesons.

TABLE 2

Anisotropy value of particles leaving the stars within different energy intervals

Energy interval of the particles in mev	π^+	π^-	without π
0-30	0.39 ± 0.08	0.22 ± 0.06	0.15 ± 0.07
> 30	0.82 ± 0.06	0.81 ± 0.05	0.82 ± 0.05
> 100	1.00 ± 0.03	0.89 ± 0.06	0.97 ± 0.03

A comparison of the data in Table 2 with results of Ref. 1 shows that, with increase in energy of the incident protons from $E_p = 460$ mev to $E_p = 660$ mev, the anisotropy of slow particles leaving the stars decreases. In Fig. 7 are shown energy distribution curves for low energy ($E < 20$ mev) particles leaving the stars under the influence of 660 mev protons. The distribution shows that the energy spectrum includes a large number of slow particles. The number of stars containing particles of energy $E < 6$ mev comprises 70% in the case of π^- meson production and about 50% in the case of stars without mesons.

Considering the fact that nuclear interactions in the photoemulsion take place principally in the nuclei of silver and bromine for which the mean Coulomb potential is ~ 9 mev relative to protons, the number of stars containing slow particles appears to be too high to be explained by the action of light nuclei, presence of subbarrier particles or the decrease of the Coulomb barrier with nuclear excitation.^{2,3} It should be noted that in emulsions which register particles of minimum ionization, it is impossible to determine effectively the mass and charge of low energy particles. Therefore, the path-energy relation

for protons was used in this work in determining the energy of particles of short paths. Thus, for example, α -particles of energy $8 < E_\alpha < 16$ mev fall into the energy interval of 2 to 4 mev. In this way, a considerable portion of the spectrum of the short path particles ($R > 40 \mu$) could be explained by the presence of α -particles of energy $E_\alpha > 8$ mev. However, it can be seen from the distribution presented in Fig. 7 that, among the rays of the stars, there is a large number of particle traces of paths shorter than 40μ which therefore must be related to particles with $Z > 2$.

3. THE MEAN FREE PATH IN THE PHOTO-EMULSION OF 660 MEV PROTONS

There were also found in this work 127 cases of interactions between protons and nuclei, registered by the method of following the protons tracks. The total length of all the traces studied was 4362 cms. Four cases were related to the elastic scattering of protons by nuclei. Thus, the mean free path of the 660 mev protons in inelastic interactions with the emission nuclei was equal $\lambda = 35.4 \pm 3.1$ cm.

The theoretical estimate of the mean free path can be obtained from the formula

$$1/\lambda_{\text{theor}} = \sum N_i \pi R_i^2 (1 - p_i), \quad (1)$$

where N_i denotes the concentration of nuclei in the i th component of the emulsion, $R_i = r_0 A_i^{1/3}$ — nuclear radius of the i th component, p_i the transparency of nuclei in the i th component. The transparency p_i was determined from the expression

$$p_i = \{1 - (1 + 2R_i/L) \times \exp(-2R_i/L)\} L^2/2R_i^2, \quad (2)$$

where L denotes the mean free path of protons in the nuclear matter.

Computation of p_i was made for two values of parameter r_0 which determines the radii of the nuclei: $r_0 = 1.2 \times 10^{-13}$ cm and $r_0 = 1.37 \times 10^{-13}$ cm.

The cross section of the interaction between the proton and the nucleons was taken as $\sigma_{np} = \sigma_{pp} = 42 \times 10^{-27}$ cm².

Results of computations of λ_{theor} are given in Table 3. As seen from Table 3, λ_{theor} , obtained for two different values of r_0 , does not differ much from λ_{exp} . It is readily shown that the dependence of λ_{theor} on σ_{np} and σ_{pp} is weaker than its dependence on r_0 [see Eq. (2)]. We can thus state that there is good agreement between the observed value of the proton mean free path in the photoemulsion and the computed value.

In conclusion we express our thanks to Prof. M. G. Meshcheriakov and Prof. V. P. Dzhelepev for the opportunity afforded us to conduct experiments with the synrocyclotron of the Institute

TABLE 3

Comparison of λ_{theor} with λ_{exper} and λ_{geom}

$r_0 \cdot 10^{13}$, in cm.	λ_{theor} , in cm.	λ_{geom} , in cm.	γ_{exp} , in cm.
1.37	37.3	25.6	35.4 ± 3.1
1.2	33.6	29.1	

for Nuclear Problems, Academy of Sciences, USSR, to L. V. Surkova, O. L. Shchipakin and G. V. Kologanova for their assistance in this work.

¹V. V. Alpers et al, J. Exptl. Theoret. Phys. (U.S.S.R.) 30, 1025 (1956).

²Le Couteur, Proc. Phys. Soc. (London) 63A, 259 (1950).

³E. Bagge, Ann. d. Phys. 33, 389 (1938).